Attenuation Curve of Galaxies at 2 < z < 7: perspectives for PRIMA

Giulia Rodighiero (University of Padova)

with

Gaia E. Esposito, Daniela Calzetti, Carlotta Gruppioni, Paolo Cassata, Pietro Benotto, Stefano Carniani

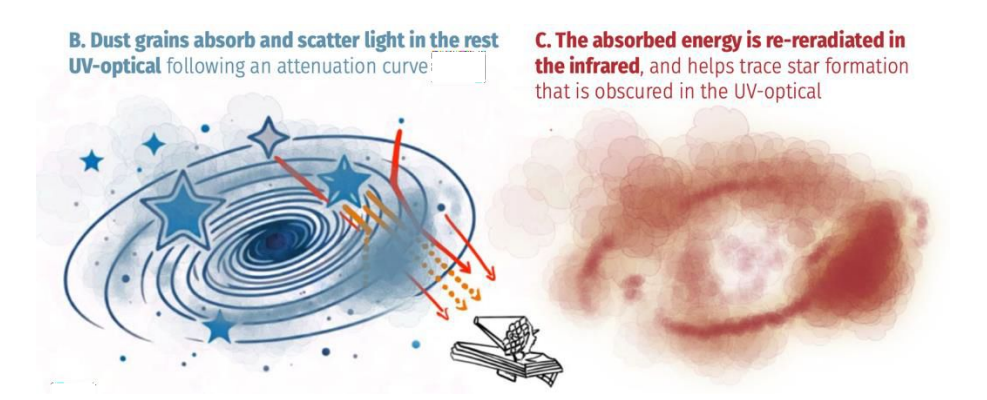
Dusty Universe 2025 (13th of November, Tucson 2025)

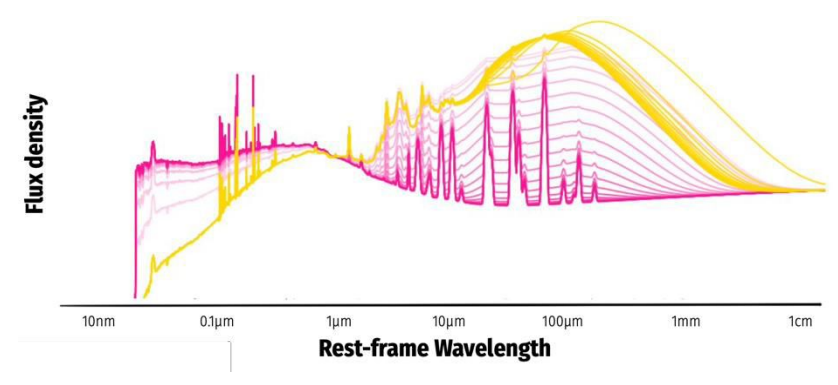


INTRODUCTION



Dust plays a crucial role in shaping galaxy spectral energy distributions (SEDs) making it difficult to interpret the fundamental properties of galaxies and limiting our understanding of their evolution.

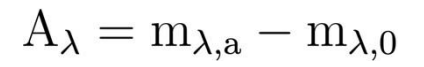




INTRODUCTION



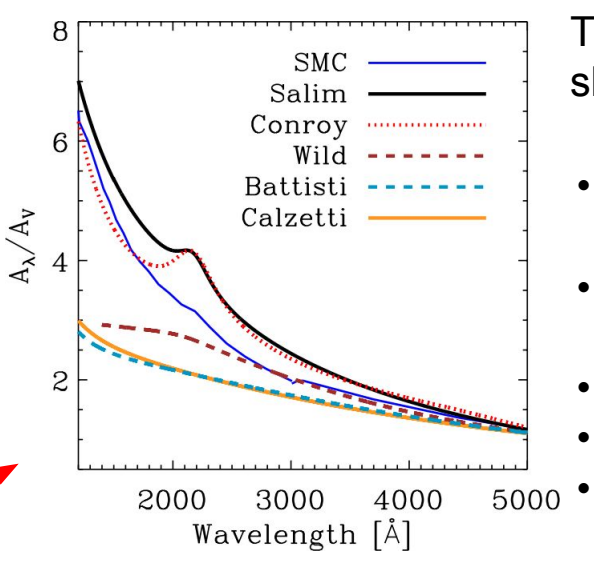
various definitions of attenuation:



Selective: $\frac{A_{\lambda} - A_{V}}{A_{B} - A_{V}}$

Total: $\frac{A_{\lambda}}{A_{B} - A_{V}}$

Absolute: $\frac{A_{\lambda}}{A_{V}}$



Salim and Narayanan (2020).

The main factors that influence the shape of attenuation curve are:

- geometrical distribution of dust inside the region;
- composition and grain size distribution of dust in the ISM;
- V-band attenuation A_V;
- metallicity Z;
 - gas mass M_{gas.}

AIM OF THE WORK



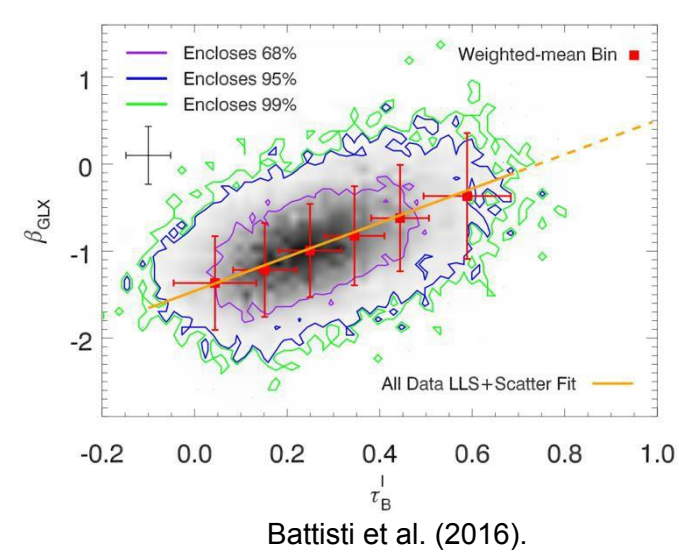
Characterize the dust attenuation law at 2<z<7 using JWST data, following the empirical method proposed by Calzetti (1994, Battisti+16).

Balmer decrement

$$au_B^l = au_{\mathrm{H}\beta} - au_{\mathrm{H}\alpha} = \ln\left(\frac{\mathrm{F}(\mathrm{H}\alpha)/\mathrm{F}(\mathrm{H}\beta)}{2.75}\right)$$

UV slope

$$F(\lambda) \propto \lambda^{\beta} \iff \beta = \frac{\log[F_{\lambda}(\text{FUV})/F_{\lambda}(\text{NUV})]}{\log[\lambda_{\text{FUV}}/\lambda_{\text{NUV}}]}$$



METHODOLOGY



- Creation of bins of Balmer Decrement, τ_B^l ;
- Average SEDs construction in each bin of τ_B^l ;
- Ratios of spectra in bins of τ_B^l (choosing a reference spectrum);
- Normalization by the difference of median values of τ_B^{ι} for each bin.

Total attenuation curve



$$\tau_{n,r}(\lambda) = -\ln \frac{F_n(\lambda)}{F_r(\lambda)}$$

$$\delta \tau_{Bn,r}^l = \tau_{Bn}^l - \tau_{Br}^l$$

$$Q_{n,r}(\lambda) = \frac{\tau_{n,r}(\lambda)}{\delta \tau_{Bn,r}^l}$$

$$Q_{n,r}(\lambda) = \frac{\tau_{n,r}(\lambda)}{\delta \tau_{Bn,r}^l}$$



$$k(\lambda) = fQ(\lambda) + R_V$$

$$f = \frac{k(H\beta) - k(H\alpha)}{E(B - V)_{star}/E(B - V)_{gas}}$$

Selective attenuation curve

$$R_V = \frac{A_V}{E(B-V)}$$

A JWST SAMPLE AT 2<z<7

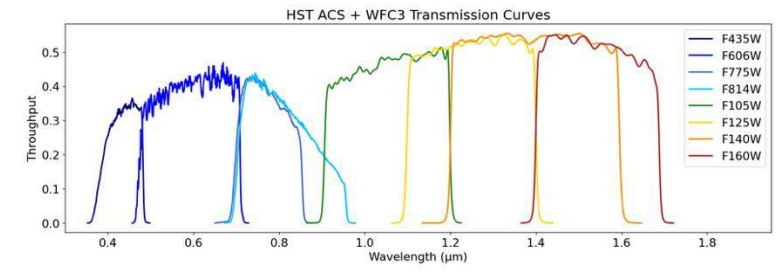


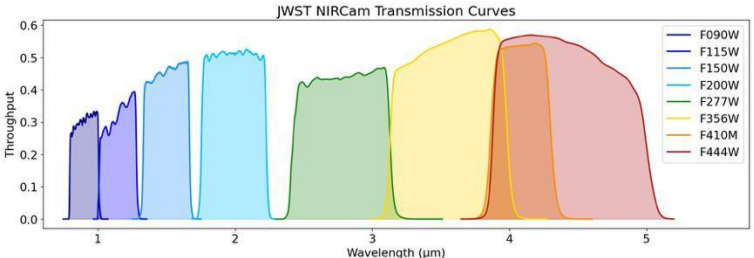
ASTRODEEP Catalog (Merlin et al. (2024)):

- NIRCam-HST multiband photometry in the GOODS fields;
- 16 filters from 0.4 μ m to 4.4 μ m;

JADES Data Release 3 (D'Eugenio et al. (2024)):

- NIRSpec/MSA spectroscopy in the GOODS fields;
- spectral range 0.6–5.3 µm;
- Medium resolution gratings (R=500-1500);
- Low-dispersion prism (R=30-300).





A JWST SAMPLE AT 2<z<7



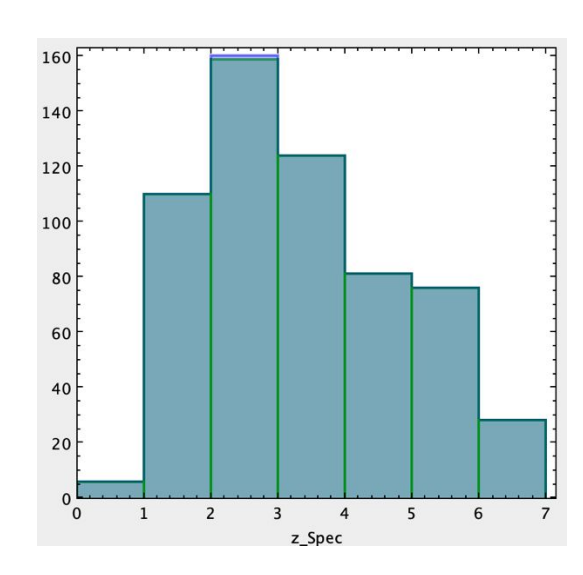
- 1. Selection targets with $H\alpha$ and $H\beta$ emission lines;
- 2. Match with photometric catalog;



534 targets

(==> **504** after appropriate slit loss corrections)

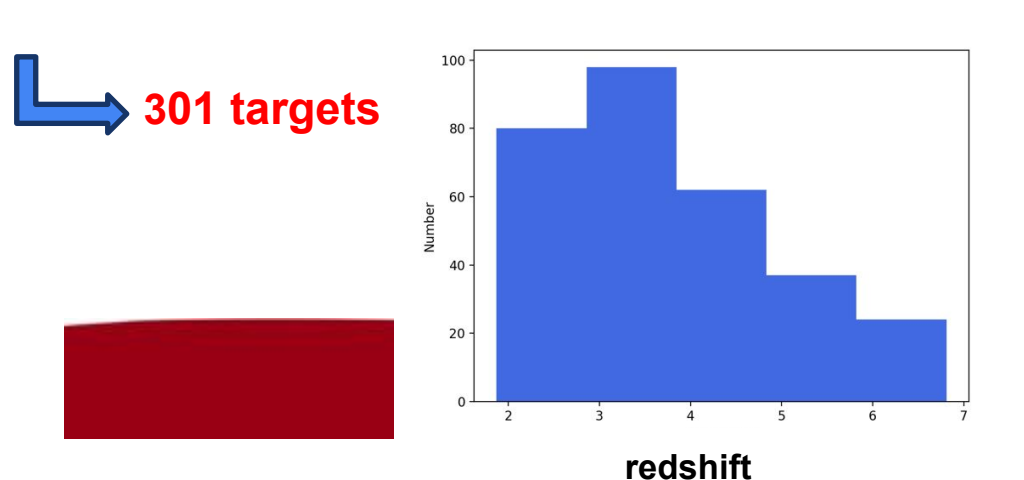


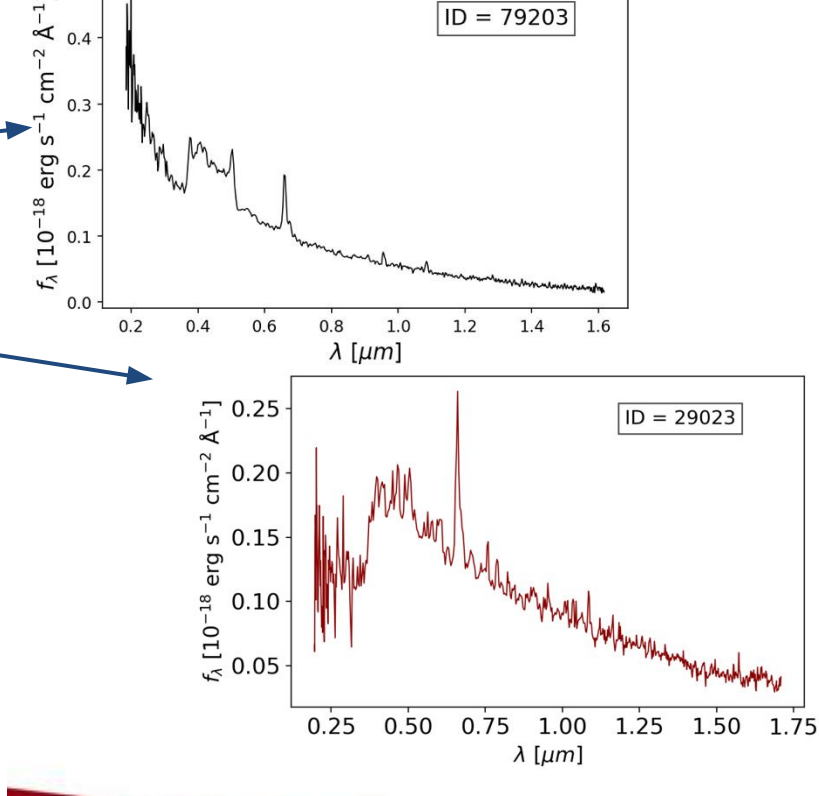


SAMPLE CUTS

Università degli Studi di Padova

- Redshift cut, z>1.84 (to probe FUV rest-frame);
- AGN removal;
- Shutter bump feature cut;
- spectra dominated by evolved stellar populations (red UV slope);
- SNR>2 at lambda<0.4um (restframe) cut.



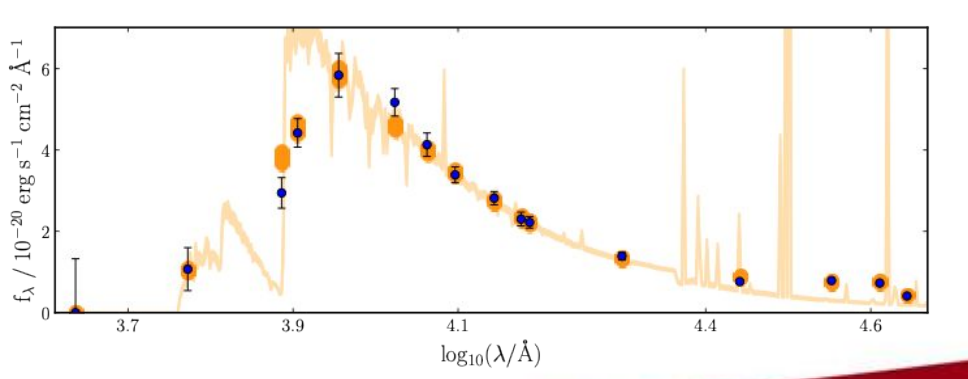


SAMPLE PHYSICAL PARAMETERS:

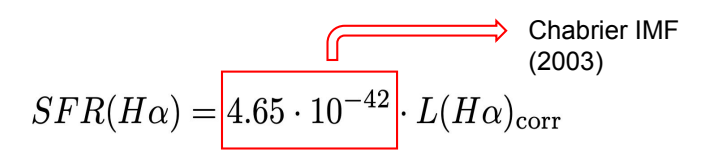


Stellar masses from BAGPIPES (Carnall+18)

| | parameters | prior | range |
|--|--|---------|-----------|
| dust | $\mathrm{A_{V}}\left[mag ight]$ | uniform | 0, 6 |
| nebular emission | $\log\!\mathrm{U}$ | uniform | -4, -1 |
| $\textbf{delayed-}\tau \ \textbf{model}$ | age [Gyr] | uniform | 0.001, 15 |
| | $	au \ [\mathrm{Gyr}]$ | uniform | 0.01, 10 |
| | ${\rm metallicity} \; [{\rm Z}_{\odot}]$ | uniform | 0, 2.5 |
| | mass-formed $[\log_{10}(M_*/M_{\odot})]$ | uniform | 6, 12.5 |



Star Formation Rates from Ha fluxes



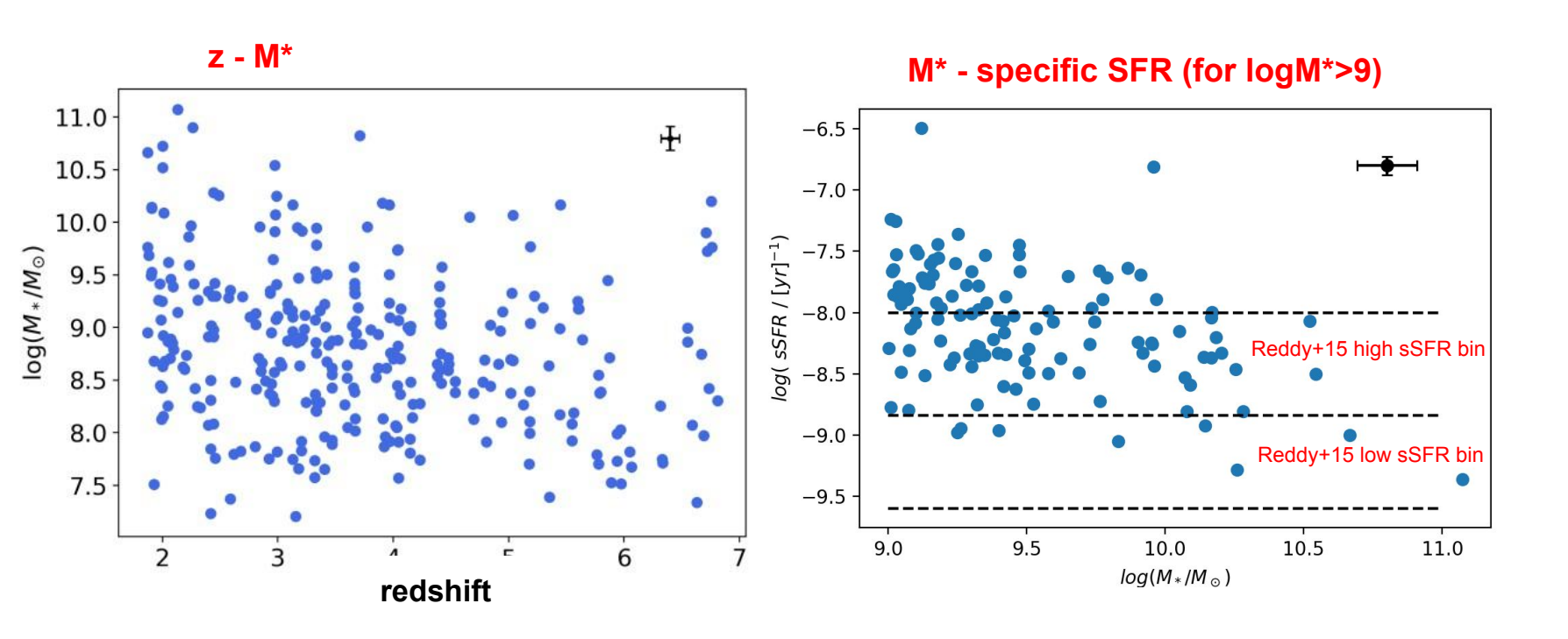
$$L(H\alpha)_{\text{corr}} = L(H\alpha)_{\text{obs}} \cdot 10^{0.4 \cdot A_{H\alpha}}$$

$$A_{H\alpha} = k(H\alpha) \cdot E(B-V)_{\rm gas}$$

$$E(B-V)_{\rm gas} = 1.086 \cdot \frac{\tau_B^l}{k(H\beta) - k(H\alpha)}$$
 Cardelli (1989) Galactic Extinction Curve

SAMPLE PHYSICAL PARAMETERS:



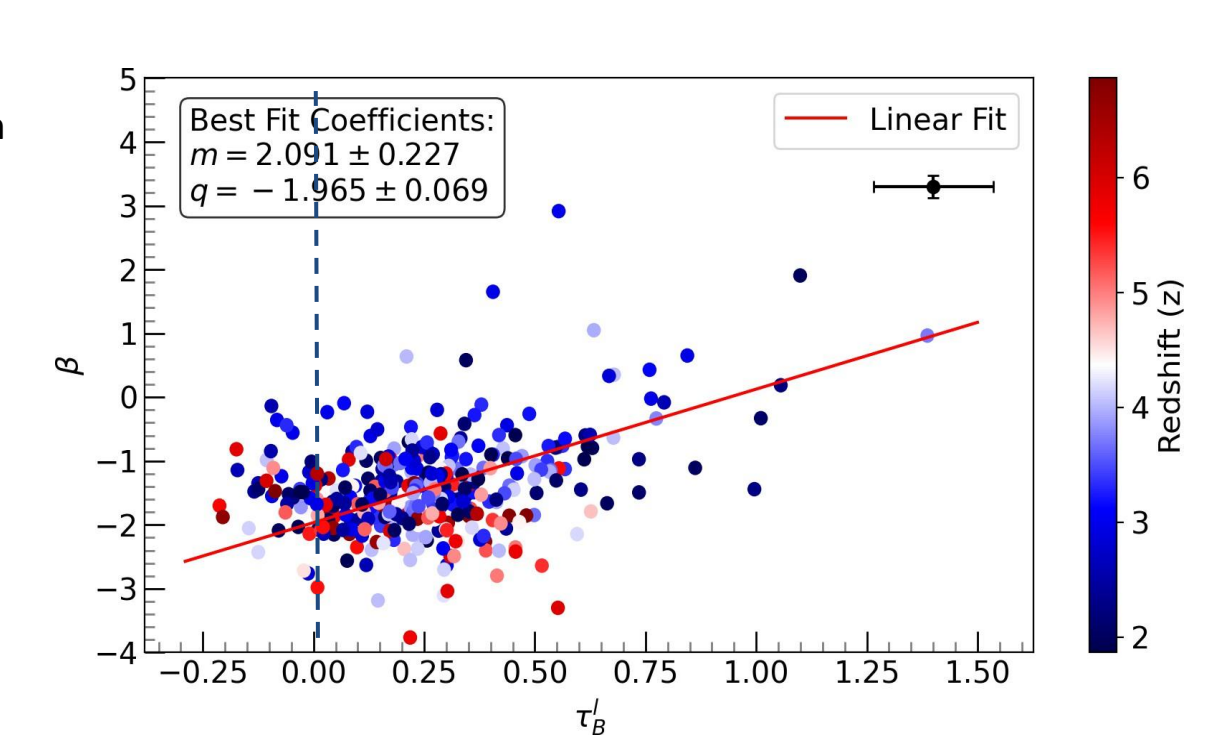


Beta-tau RELATION



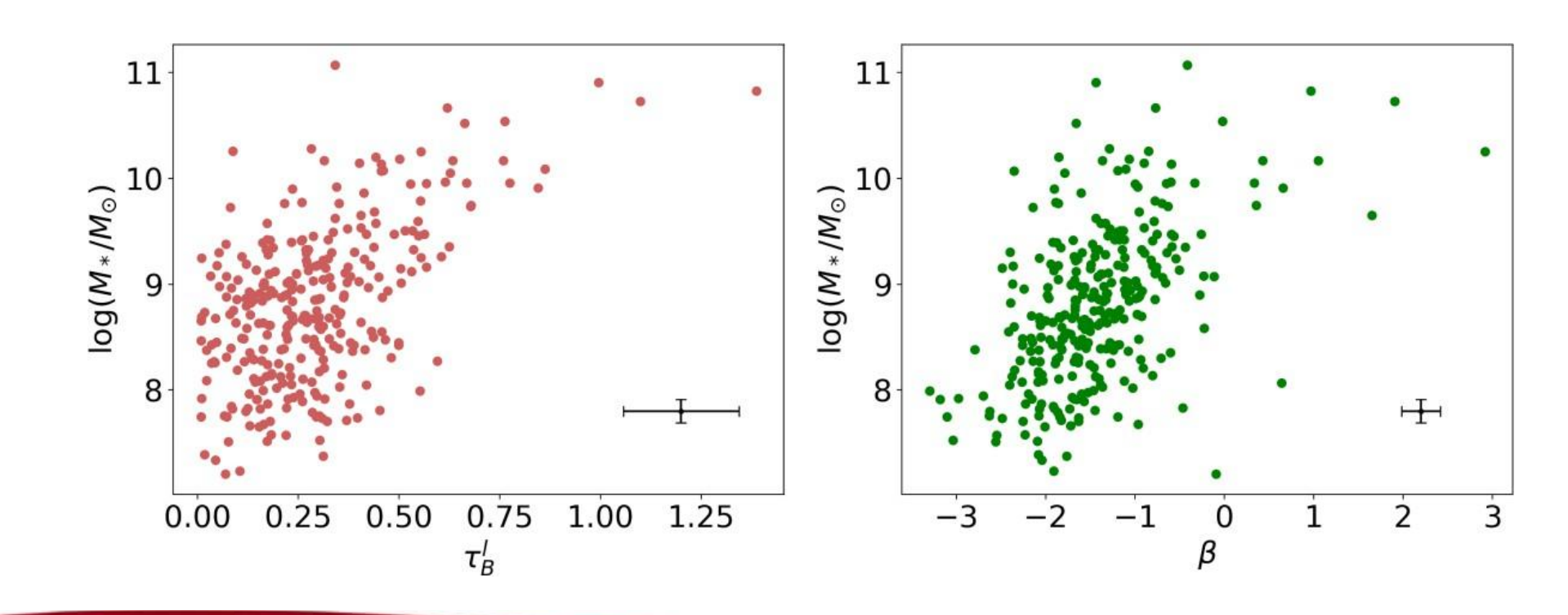
 FUV and NUV restframe fluxes estimates with a linear interpolation between fluxes in the nearest photometric bands;

$$\beta = \frac{\log[F_{\lambda}(\text{FUV})/F_{\lambda}(\text{NUV})]}{\log[\lambda_{\text{FUV}}/\lambda_{\text{NUV}}]}$$



SAMPLE PHYSICAL PARAMETERS:

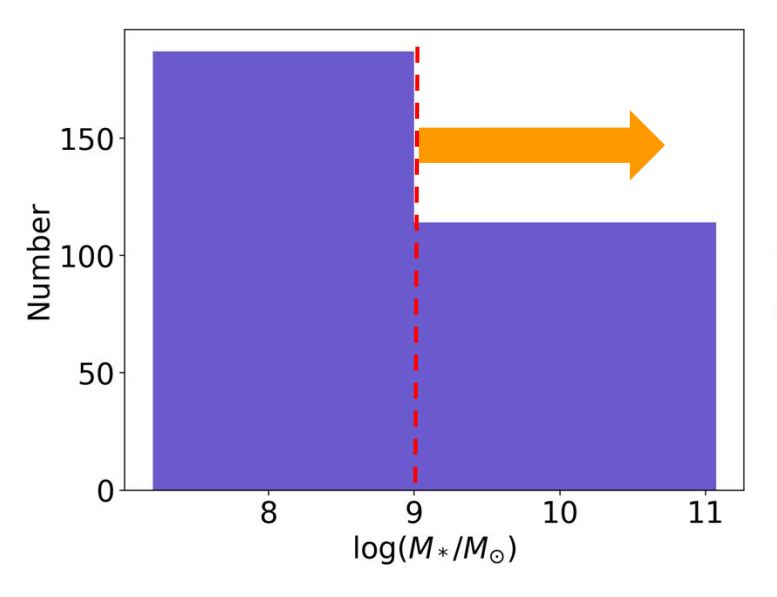




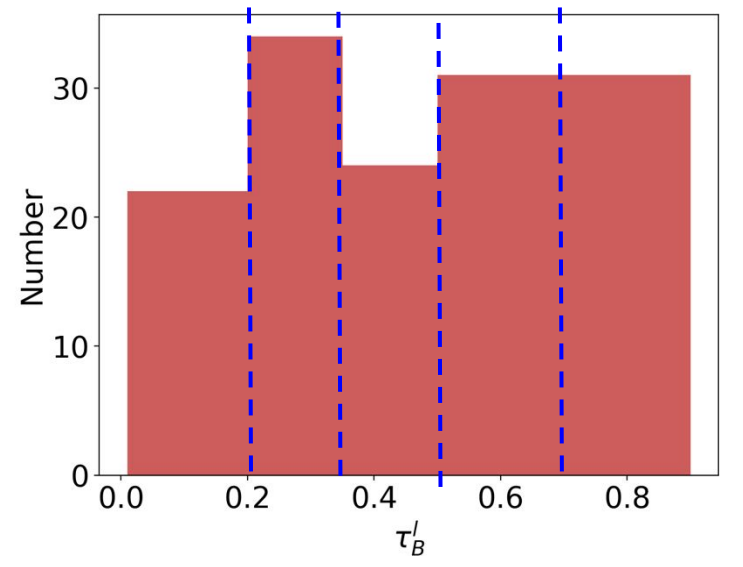
we limit our analysis to log(M*/Msun)>9 and we populate 5 Balmer Decrement bins







Balmer Decrement distribution at log(M*/Msun)>9



AVERAGE SEDs



- 1. Shift of the spectra to rest-frame for each target;
- 2. Removal of emission lines;
- 3. Selection of the wavelength range common to all targets;
- 4. Regridding to bring all the spectra to the same resolution;
- 5. Normalization by the flux value at 5500Å;
- 6. Stacking of the spectra.



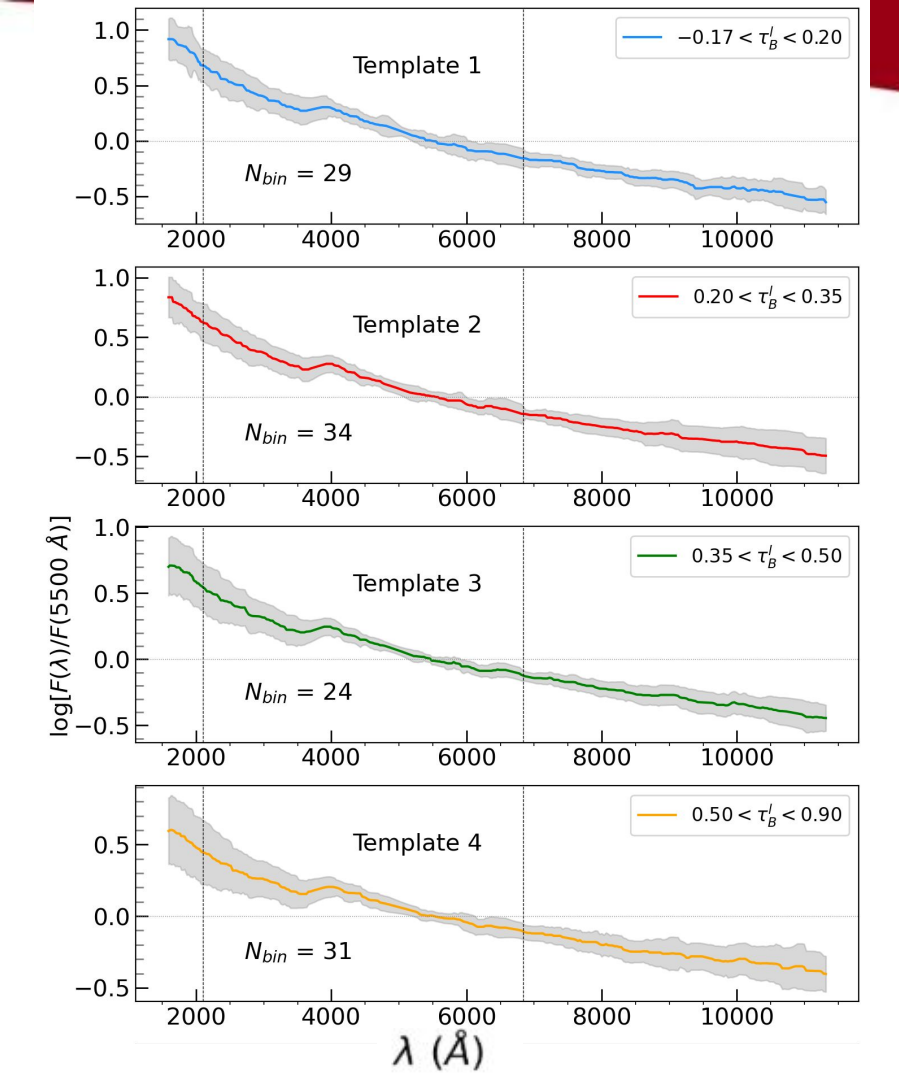
Three different spectral regions:

- $1600 \text{ Å} < \lambda < 2100 \text{ Å} \to 50\% \text{ sample}$
- 2100 Å < λ < 6800 Å \rightarrow full sample
- $6800 \text{ Å} < \lambda < 11400 \text{ Å} \to 50\%$ sample

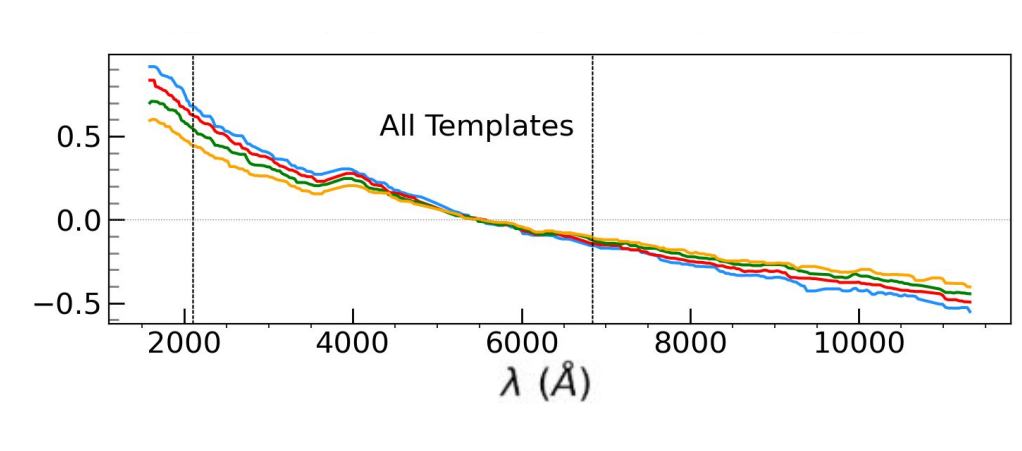
Single continuous average SED



Smoothing with a median filter

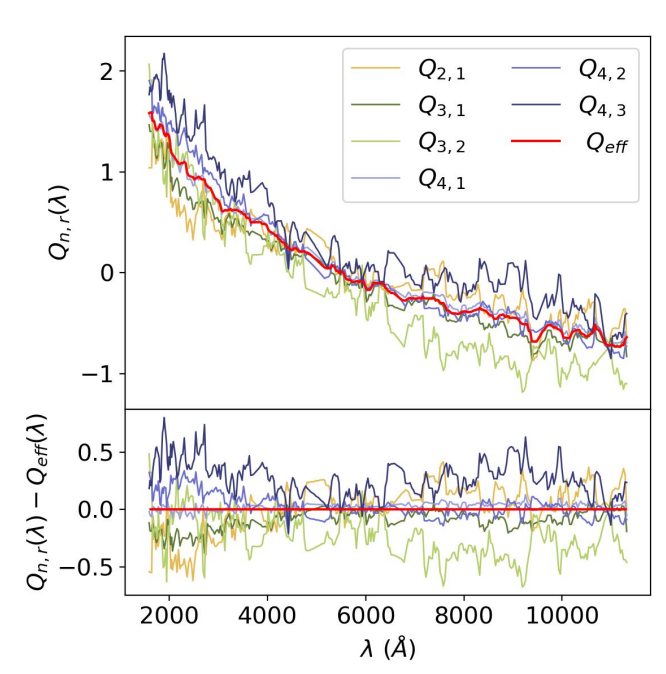


AVERAGE SEDs



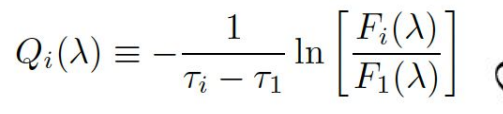
UV-eta slope becomes redder as au_B^l increases.

SELECTIVE ATTENUATION CURVE



consistent with:

- high sSFR by Reddy+15 at z=2
- Battisti+2022 at z=1.3

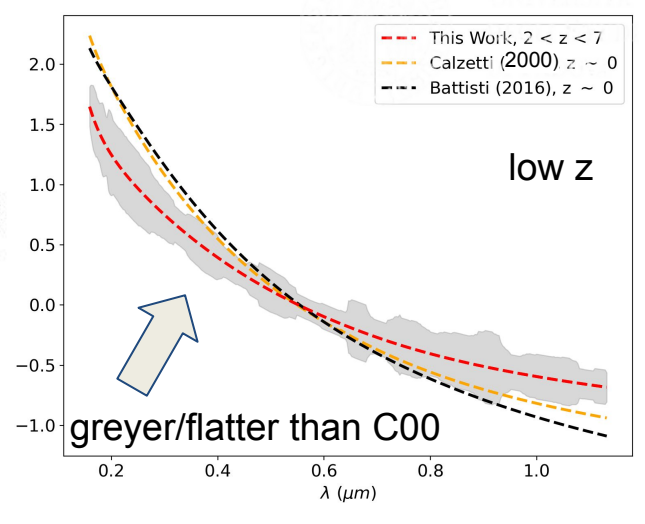


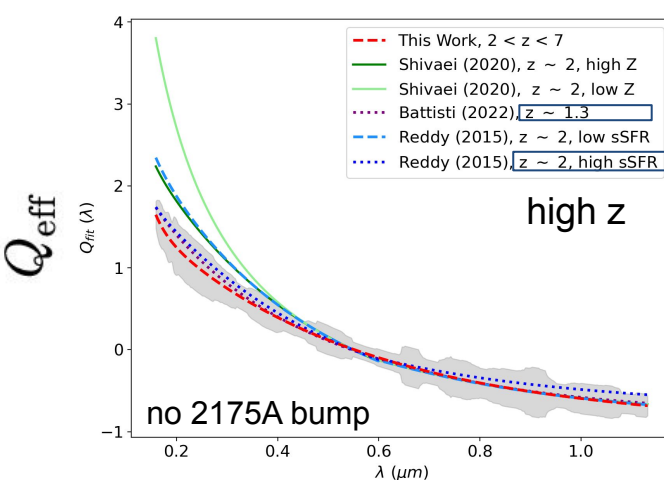
The definition of Q implies that the Balmer optical depth is related to the difference in optical depths of the continuum at the wavelengths of H(alpha) and H(beta) (Reddy+15)

polynomial interpolation

⇒

comparison with local and high-z attenuation measurements





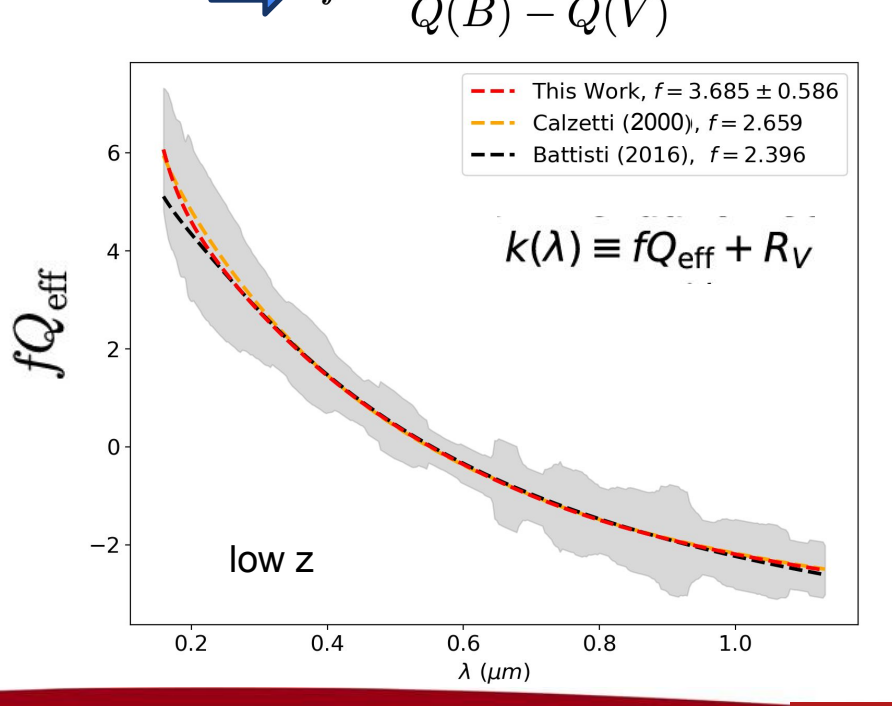
SELECTIVE ATTENUATION CURVE ⇒ stellar continuum

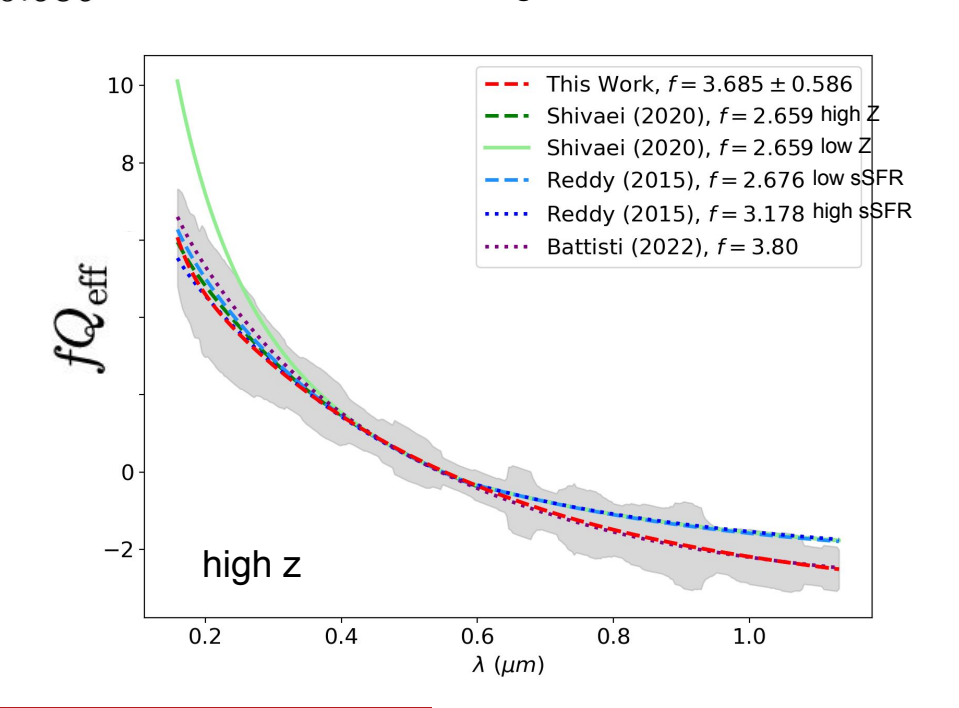


E(B-V)=A(B)-A(V) &
$$k(\lambda) = \frac{A_{\lambda}}{A_{B} - A_{V}}$$
 $k(B) - k(V) \equiv 1$

$$f = \frac{1}{A_{A} - A_{V}} = 3.685 \pm 0.586$$

when accounting for the nebular-to-continuum correction factor (f), most curves gets consistent





ABSOLUTE ATTENUATION CURVE ⇒ requires Rv normalization



$$A_{\lambda}/A_{V} = k_{\lambda}/R_{V} \quad k(\lambda) = fQ(\lambda) + R_{V} \qquad \text{Several assumption on RV} \\ \text{(not constrained, yet, by observations)} \\ k(\lambda \to \infty) = 0 \quad R_{V} = 4.00 \pm 0.66 \qquad \text{extrapolated} \\ \\ R_{V=3.0} \quad \text{MW} \quad \text{Gordon (2003)} \\ \text{RV=4.00} \quad \text{MW} \quad \text{Gordon (2003)} \\ \text{RV=5.0} \quad \text{This Work} \quad \text{RV=4.00} \\ \text{This Work, RV = 4.0} \quad \text{RV=4.05} \\ \\ \\ A_{L}\mu m \\ \text{higher normalization than Reddy+15} \\ \text{@z} \sim 2$$

 The average selective attenuation curve for massive galaxies, Q(λ), at 1.8<z<7 is flatter (greyer) than the local relation by Calzetti+00 and Battisti+16. Larger dust grains?

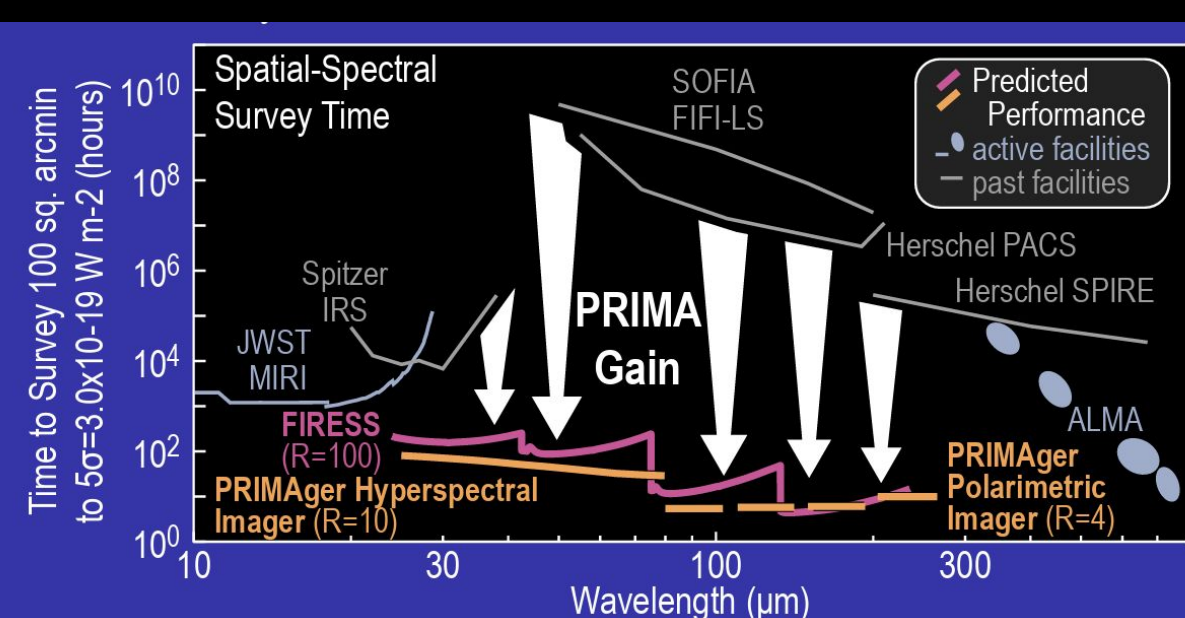
- No 2175 A bump is detected.
- At higher z, it is consistent in the UV with the results of Reddy et al. (2015) at z~2 and Battisti et al. (2022) at z~1.3, whose samples span stellar masses and sSFR ranges similar to ours. In contrast, it differs from studies based on samples with lower sSFRs ⇒ hints for a potential strong dependence on sSFR.
- the normalized attenuation is instead consistent and flat as the Calzetti one.
- Scenario in which young stars, affected by both birth-cloud and ISM dust, contribute more strongly, producing an optically thicker medium.
- The attenuation curves Q(λ) derived in different redshift bins are consistent with each other, suggesting **no clear redshift evolution**.
- Metallicity dependences have not been evaluated.

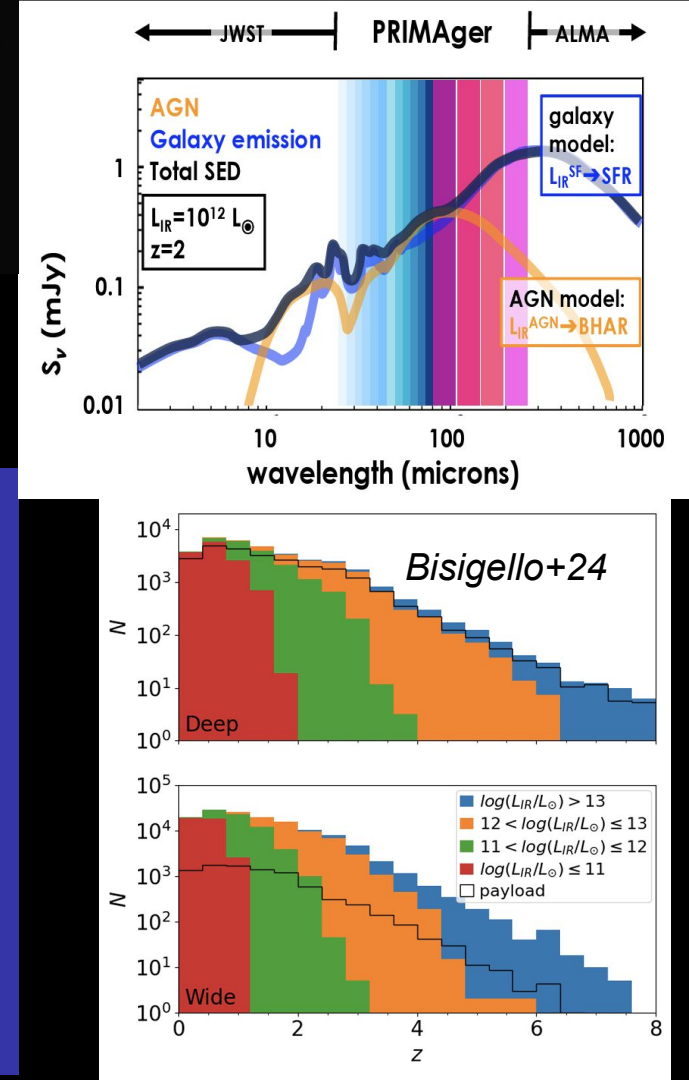
Future perspectives:

PR'MA

Mid-to-far Infrared detection of sources used to measure attenuation law

- 1) direct constraints on Rv
- 2) direct identification of the UV bump





Thank you!

